

Nickel Foam Based Phase Change Materials with Excellent Performances

Lifei Chen, Xin Wang

School of Energy and Material Engineering, Shanghai Polytechnic University
2360 Jinhai Road, Pudong District, Shanghai, China
lfchen@sspu.edu.cn, wangxin@sspu.edu.cn

Abstract - Phase change thermal storage technology is important for the efficient utilization and conversion of thermal energy resources, but problems such as easy leakage and low thermal conductivity greatly limit its application in thermal energy storage. In this study, a novel foam-based composite phase change material (CPCM) was successfully prepared by vacuum impregnation and melt blending process using n-octadecane as the phase change material, porous nickel foam as the carrier, and metal nanoparticles/carbon nanotubes (M-NPs@CNTs) as the thermally conductive fillers. The effects of the type and content of M-NPs@CNTs on the properties of CPCM were also investigated. The results show that CPCM has good shape stability, excellent thermal conductivity ($2.01 \text{ W}\cdot\text{m}^{-1}\cdot\text{K}^{-1}$) and excellent thermal energy storage capacity (182.5 J/g), and has a wide range of applications.

Keywords: Phase change thermal storage; Thermally conductive fillers; Foam metal; Composites

1. Introduction

Thermal energy is an indispensable energy source for social development, and thermal storage and thermal management are of great significance for the efficient and safe utilization of thermal energy resources [1,2]. Phase change thermal storage technology utilizes the phase transition of phase change materials (PCMs) to realize the storage and release of thermal energy, which has the characteristics of strong thermal storage capacity, simple process, and green environmental protection, and it can be widely used in the fields of industrial waste heat recovery, solar energy utilization, and energy-saving buildings [3,4]. Among them, PCM, as a smart material, is an ideal carrier for thermal energy storage with the advantages of strong energy storage and release capacity, high chemical stability, reusability and abundant natural resources [5]. However, some inherent defects limit the use of PCMs, such as low thermal conductivity and susceptibility to leakage during phase transition, which severely limit their application in energy conversion and storage systems. Therefore, a lot of efforts have been put into the design and fabrication of shape-stabilized composite phase change materials, ranging from microcapsules and porous scaffolds absorption to chemically grafted and cross-linked compounds [6,7]. For example, Xu Zong [8] prepared foam-based composite phase change materials by melt impregnation and casting methods with different foam metals as carriers and paraffin wax as phase change material. The thermal conductivity and temperature field variations of the foam-based composite phase change materials were investigated. The comparative experimental results show that the foam-based composite phase change materials with copper foam and nickel foam as the thermal conductive carriers and paraffin wax as the phase change material have more stable heat storage capacity and more uniform temperature field distribution. The heat transfer stability and thermal conductivity of the foam-based composite phase change material with copper foam as the thermal conductive carrier and paraffin wax as the phase change material are optimal.

Foam matrix composites (FMCs) are new multifunctional lightweight composites with low density, high strength, large specific surface area and high surface energy, which have a wide range of applications in many fields such as chemical industry, energy storage, military and aerospace [9,10]. Therefore, in order to improve the performance of energy conversion and storage systems, the pore structure of foam-based composites and their capillary adsorption are utilized to prepare foam-based composite phase change materials (CPCMs) by combining them with PCMs and building fast thermal conduction channels in synergy with heat-conducting fillers, which can realize the efficient transfer and storage of heat [11,12]. CPCMs utilize porous foam metal as a carrier for the PCM for adsorption, which not only can confine the PCM firmly in its porous structure to achieve the effect of encapsulation and shaping, but also effectively solves the problems of easy flow and volume

change during the solid-liquid phase transition of PCM [13]. Meanwhile, the thermal conductive materials are doped into the CPCM, and the high thermal conductive fillers such as carbon fiber, carbon nanotubes, graphene and McElene are utilized as additives, which can effectively improve the thermal conductivity of the composites and promote the photothermal conversion [14]. Among them, multi-walled carbon nanotubes (MWCNTs) have excellent properties such as high mechanical strength and high thermal conductivity, which are the first choice for thermally conductive reinforcement materials. However, MWCNTs are surface inert and easily agglomerated in the matrix, which seriously affects practical applications [15]. Therefore, metal nanoparticles (M-NPs) are modified on the surface of MWCNTs using pyrolysis, which not only can avoid CNTs agglomeration and improve their dispersion, but also can utilize M-NPs to construct heat transfer channels between CNTs, reduce the contact thermal resistance between CNTs, and obtain composite thermally conductive fillers with excellent thermal conductivity properties. In summary, in this study, a novel foam-based composite phase change material (CPCM) was successfully prepared by vacuum impregnation and melt blending process, using n-octadecane as phase change material, porous nickel foam as carrier, and metal nanoparticles/carbon nanotubes (M-NPs@CNTs) as thermally conductive filler, and the resulting samples have good thermal conductivity with high heat storage density.

2. Experimental section

2.1. Materials and apparatus

N-octadecane (C18) was purchased from Sinopharm Group Chemical Reagent Co. Ltd, nickel foam (NF) was purchased from Kunshan Shengshi Jingxin New Material Co. Ltd, AgNPs/CNTs (self-manufactured), CoNPs/CNTs (self-manufactured), NiNPs/CNTs (self-manufactured), anhydrous ethanol was purchased from Sinopharm Group Chemical Reagent Co.

A scanning electron microscope (Hitachi S4800) was used to observe the morphology and microstructure of the CPCM, and the chemical structure of the CPCM was analyzed by a Tensor27 FT-IR spectrometer. A D8-Advanced X-ray diffractometer operating at a scanning rate of 20°/min over a scanning range of 20-80° was used to reveal the crystalline structure of the CPCM. The CPCM's latent heat properties were measured by differential scanning calorimeter (pyris 1 DSC). This was carried out under nitrogen-protected conditions in the temperature range of 10-50 °C with the heating and cooling rates set to 5 °C/min. Thermogravimetric analysis of the thermal stability of CPCM was tested under nitrogen-protected conditions in the temperature range of 25-600°C with a heating rate of 10°C/min. The thermal conductivity of the composites was measured three times using a thermal conductivity tester (C-Therm) and the average of the three times was taken.

2.2 Preparation of C18/M-NPs@CNTs/NF stereotyped composite phase change materials

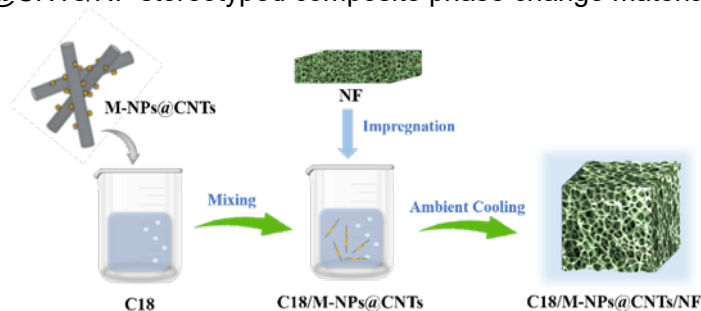


Fig. 1 Schematic diagram of the preparation process of CPCM

The C18/M-NPs@CNTs/NF composite phase change materials were prepared by a combination of melt infiltration and vacuum impregnation methods, and the preparation process is shown in Fig. 1. A certain proportion of C18 was placed at the bottom of the beaker, and carbon nanotubes (M-NPs@CNTs) composite thermally conductive fillers loaded with different metal nanoparticles as well as MWCNTs unloaded with M-NPs were weighed into the beaker, which was dispersed by ultrasonication to make a homogeneous mixture with the solvent, and then heated and stirred for 30 min at 70 °C. With the increasing temperature, the phase change material gradually melted and mixed with the M-NPs/CNTs composite thermally conductive filler uniformly, and then the NF was put into the heated beaker and impregnated for 10 minutes. The beaker was then placed in a vacuum drying oven for another 10 min, and then the composite phase change material was

immediately removed and cooled to room temperature. The samples obtained by this method were named C1, C2, C3, C4, C5, C6, C7, C8, C9, respectively.

Table 1: Composition of prepared samples

Sample	C18 (g)	NF (g)	NiNPs/CNTs (g)	CoNPs/CNTs (g)	AgNPs/CNTs (g)
C ₁	2.0345g	0.1451	0.0198	0	0
C ₂	1.9995g	0.1518	0.1188	0	0
C ₃	2.1029g	0.1380	0.1994	0	0
C ₄	2.1243	0.1434	0	0.0380	0
C ₅	2.2106	0.1434	0	0.1020	0
C ₆	2.0953	0.1414	0	0.2005	0
C ₇	3.7613	0.1500	0	0	0.0444
C ₈	3.9000	0.1417	0	0	0.1154
C ₉	3.6888	0.1438	0	0	0.2185

3. Results and discussion

3.1. Morphological structure of C18/M-NPs@CNTs/NF composite phase change materials

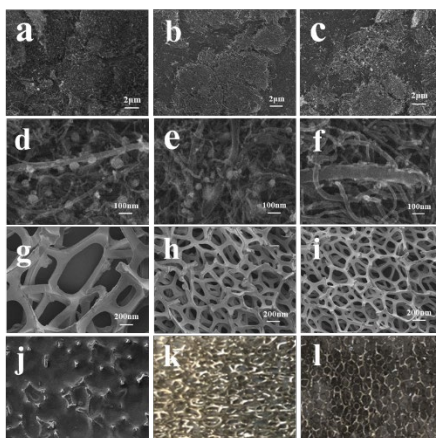


Fig. 2 SEM images and microscope images of samples : (a, d) NiNPs@CNTs, (b, e) CoNPs@CNTs, (c, f) AgNPs@CNTs 8K, (g)40PPI NF,(h)70PPI NF, (i, k)110PPI NF,(j, l) AgNPs@CNT/C18/110PPI NF.

The microstructures of NiNPs@CNTs, CoNPs@CNTs, and AgNPs@CNTs are shown in Fig. 2(a-f). Fig. 2(k-l) shows the microscope pictures of NFs without C18/M-NPs@CNTs added and CPCM with C18/M-NPs@CNTs added. The MWCNTs with hollow structures can be clearly seen in the figure as curved and haphazardly entangled. Among them, the M-NPs@CNTs samples were prepared by ball-milling a mixture of metal acetate and MWCNTs using heat treatment. The test results showed that the M-NPs were uniformly distributed on the surface of MWCNTs. With the same loading of M-NPs, the average particle size of M-NPs/CNTs samples obtained by ball milling and mixing method followed by heat

treatment was smaller than that of the samples prepared by milling and mixing. The reason for this is that ball milling can improve the surface defects of MWCNTs, which makes the active sites for M-NPs to grow in MWCNTs increase, the number of particles increases, and the corresponding particle radius becomes smaller. As can be seen from Fig. 2(g-i), NF has a rich pore structure, which provides abundant adsorption space for the incorporation of phase change materials. Compared with the microstructure of NF, the composites of C18 and NiNPs@CNTs are uniformly filled in the NF lattice structure, presenting a mechanically interconnected structure, and NiNPs@CNTs can effectively prevent the leakage of C18.

3.2. Chemical structure of C18/M-NPs@CNTs/NF composite phase change materials

The Fourier total reflection infrared spectra (ATR-FTIR) of C18 and C18/M-NPs@CNTs/NF are shown in Figure 3(a). The test curves of C18, 10 wt% AgNPs@CNTs, 10 wt% CoNPs@CNTs, C4, C5, and C7-C9 are represented in Fig. 3(a), respectively. As can be seen from Fig. 3 (a) , all samples have similar three characteristic absorption peaks:

- 1) near 2920 cm^{-1} and 2850 cm^{-1} are the stretching vibrational absorption peaks of $-\text{CH}_2-$,
- 2) near 1472 cm^{-1} is the bending vibrational absorption peak of $-\text{CH}_3-$,
- 3) near 716 cm^{-1} is the rocking vibration peak of $-(\text{CH}_2)_n-$ ($n \geq 4$).

The characteristic absorption peaks of C18 are consistent with the positions of the corresponding peaks at 2920 cm^{-1} , 2850 cm^{-1} , 1472 cm^{-1} , and 716 cm^{-1} . As can be seen from Fig. 3(a), no new IR absorption peaks appeared in the samples and there was no significant shift in the IR absorption peaks. Therefore, the results of IR absorption spectra proved that no new substances were generated between C18 and NF, only molecular forces existed, the two materials were chemically compatible and no new chemical bonds were generated due to the chemical reaction, and the prepared composite phase-change materials could maintain stable phase-change properties. Meanwhile, the IR characteristic curves of C18/M-NPs@CNTs/NF composite phase change materials all have the above characteristic absorption peaks of n-octadecane, indicating that C18 has been adsorbed by NF. And it can be seen in the curves of C4, C5, C7-C9 that the intensity of the peaks at 2850 and 2920 cm^{-1} in the middle is weaker than that of C18, which can also indicate that the NF has adsorbed C18 well.

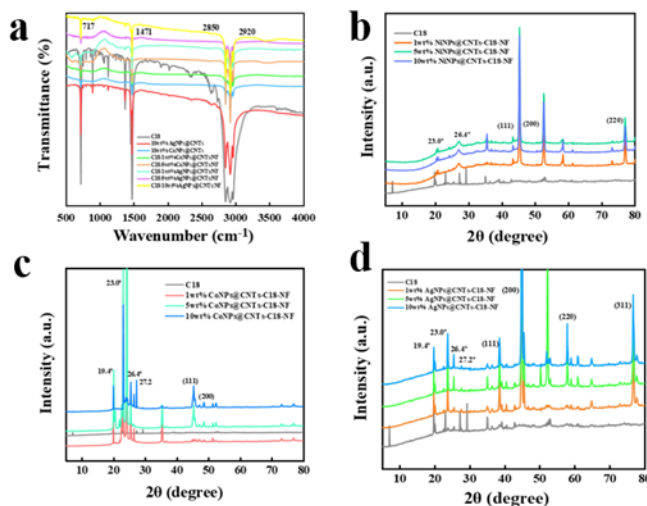


Fig. 3 (a) FTIR spectra of C18 and 10 wt% AgNPs@CNTs, 10 wt% CoNPs@CNTs, C4, C5, C7-C9 (b) XRD plots of C18, C1-C3 (see Table 2) (c) XRD plots of C18, C4-C6 (d) XRD datasheets of C18, C7-C9.

3.3. Crystal structure of C18/M-NPs@CNTs/NF composite phase change materials

Figures 3(b), (c) and (d) show the XRD patterns of C18, C1-C9, respectively. As shown, sharp diffraction peaks of C18 were observed at about $2\theta = 23.0^\circ$ and 27.2° , while classical diffraction peaks of MWCNTs were observed at $2\theta = 26.4^\circ$. In addition, the characteristic diffraction peaks at $2\theta = 44.52^\circ$, 51.88° , and 76.4° correspond to the (111), (200), and (220)

crystal planes of NiNPs, respectively; the characteristic diffraction peaks at $2\theta = 44.4^\circ$ and 51.8° correspond to the (111), and (200) crystal planes of CoNPs, respectively; and the characteristic diffraction peaks at $2\theta = 37.8^\circ, 44.6^\circ, 64.8^\circ,$ and 77.1° correspond to the characteristic diffraction peaks of the (111), (200), (220), and (311) crystal planes of AgNPs, respectively. C1-C9 and C18 show the same diffraction peaks of C18. The high content of C18 in the CPCM and the skeleton filled with C18 may be the cause of the disappearance and weakening of the C18 diffraction peaks. The results show that simple physical mixing has no effect on the crystal structure of C18/M-NPs@CNTs/NF composites.

3.4. Stability of C18/M-NPs@CNTs/NF composite phase change materials

In order to consider the thermal stability of C18/M-NPs@CNTs/NF composite phase change materials, the samples were tested for leakage. First, the prepared samples were placed in a glass dish lined with weighing paper, and the mass of CPCM was weighed and recorded first. Then the CPCM was placed in an oven at 60°C and the leakage of C18 from the sample was recorded every 30 minutes for a total of 600 minutes of testing. The mass of the CPCM after being put into the oven was subtracted from the mass of the CPCM before being put into the oven to characterize the leakage mass of C18 in the sample. The test results are shown in Figure 4(a).

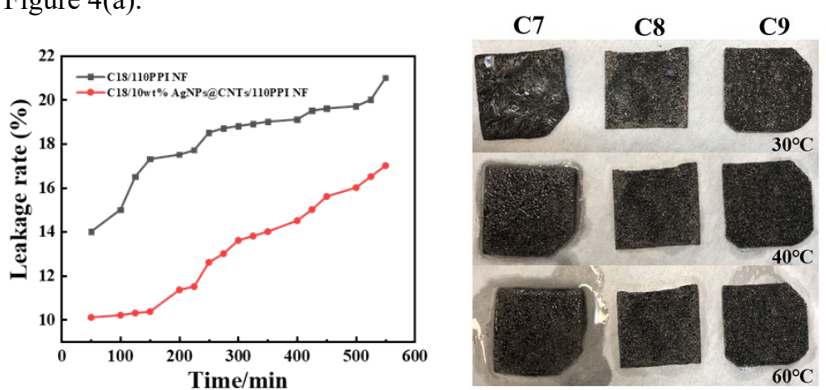


Fig. 4 (a) C18/110PPI NF and leakage test before and after addition of 10wt% AgNPs@CNTs. (b) Leakage testing of C7-C9 composites at different temperatures.

The shape stability of CPCM is very important in practical applications because it effectively prevents the leakage of the phase change material when it transforms from solid phase to liquid phase. A comparative study of the shape stability of C7-C9 was carried out by directly observing the shape evolution of the phase change material during the melt phase change. Figure 4b shows the leakage change process of C18 in the tested sample when heated in the oven. The experimental results show that the leakage of C18 is relatively large after several cycles. Before adding AgNPs@CNTs, after 19 cycles (600 minutes), the leakage of C18 was approximately 21.00%. After adding AgNPs@CNTs, the leakage of C18 was approximately 17.2%. Within the error range, it can be considered that the addition of AgNPs@CNTs reduces the leakage of C18 by approximately 3.8%. Using NF as a carrier reduces the leakage rate of C18. The M-NPs@CNTs are filled into the NF-rich pore structure, which creates a certain resistance to the melting and leakage of C18, reducing the leakage rate of C18.

It is clearly observed from Fig. 4(b) that the pure C18 gradually melted with the heating time, and the molten C18 completely melted into liquid flowing around at 60°C . And the C18/M-NPs@CNTs/NF composites showed good shape stability throughout the heating process. Only very little molten C18 was observed at the bottom of both C18/10wt%AgNPs@CNTs/NF composite samples, which was caused by the adsorption of C18 on the sample surface. Notably, the C9 composite (right) shows less leakage of molten C18 than that of C7 (center), suggesting better immobilization of molten C18. The results demonstrate that the C18/M-NPs@CNTs/NF composite C18 can maintain good shape stability when undergoing solid-liquid phase transition.

3.5. Phase transition heat storage in C18/M-NPs@CNTs/NF composite phase transition materials

The phase transition temperatures and phase transition latent heat values of the samples were measured by DSC, as shown in Fig. 6 (a-c). Compared with pure C18, the melting points of C1-C9 are all reduced. The first phase transition process

occurs at 36.6 °C, which corresponds to the solid-liquid phase transition process of solid C18 during heating. As can be seen in Table 2, the melting peak temperature of C9 composite phase change material slightly decreases from 38.17°C to 35.84°C compared to C18, which is attributed to the introduction of M-NPs@CNTs, which has a high thermal conductivity, and the CPCM has a more sensitive thermal response property. The M-NPs@CNTs particles act as thermally conductive reinforcing materials and do not undergo any phase change behavior. Therefore, the latent heat value of the phase transition of the samples decreases continuously with the increase of the mass fraction of M-NPs@CNTs, and the latent heat value of C9 decreases from 223.2 J/g to 160.5 J/g, which is a decrease of 28%. The reason for this phenomenon is that C18 plays a major role in the thermal energy storage of the sample, not the more amount of doped M-NPs@CNTs can enhance the latent heat capacity of the whole system, but rather, the excessive amount of M-NPs@CNTs has a certain counter effect on the latent heat capacity of the sample. In summary, when the content of M-NPs@CNTs is added as 1 wt%, the latent heat value of C18/M-NPs@CNTs/NF definite composite phase change material is the largest, which is 182.5 J/g. When the doped thermally conductive fillers are AgNPs@CNTs, the latent heat value of the phase change of the CPCM are larger than that of the thermally conductive fillers are NiNPs@CNTs, CoNPs@CNTs of the CPCM.

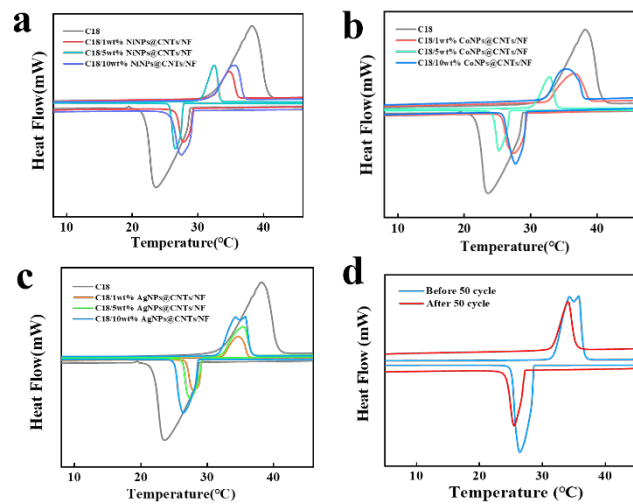


Fig. 6 (a) DSC profiles of C18 and samples during the melting and solidification phases: (a) C1-C3 (b) C4-C6 (c) C7-C9 (d) C9 before and after 50 thermal cycle treatments.

Table 2 DSC data for C18 and C1-C9

Samples	C18	C ₁	C ₂	C ₃	C ₄	C ₅	C ₆	C ₇	C ₈	C ₉
T(°C) ^a	31.34	31.17	29.67	30.84	31.17	30.00	30.84	30.50	30.17	31.17
T(°C) ^b	38.17	34.84	32.50	35.50	36.67	32.84	35.50	34.67	35.34	35.84
T(°C) ^c	40.84	36.34	33.50	37.50	39.00	34.34	38.17	36.50	37.00	37.34
H _{Melting}	223.2	155.59	149.7	146.6	160.7	158.4	140.1	182.5	172.8	160.5

Note: a: temperature at which melting begins; b: peak melting temperature; e: temperature at which melting ends.

3.6. Cyclic stability of C18/M-NPs@CNTs/NF composite phase change materials

To demonstrate the cycling stability of CPCM, solid-liquid phase transition cycling tests were measured by DSC. Figure 6(d) shows the latent heat properties of C9 before and after 50 thermal cycle treatments. It can be seen that the 50 thermal cycling treatment did not change the phase transition latent heat properties significantly for C9. The melting and crystallization temperatures of C9 varied within a narrow range. The fluctuation of the phase transition temperature is only

about 0.1 °C, and the fluctuation of the phase transition latent heat value is less than 1%, i.e. almost constant. These reasonable and acceptable variations in temperature and latent heat indicate that the as-produced CPCM is reliably thermally stable after extensive thermal cycling.

3.7. Thermal conductivity of C18/M-NPs@CNTs/NF composite phase change materials

Figure 7(a-d) shows the thermal conductivities of C18, C1-C9, which are 0.35, 1.83, 2.35, 2.71, 1.88, 2.49, 2.76, 2.01, 2.56, and 2.80 W/(m·K), respectively. The test results showed that the thermal conductivity of C9 was 699% higher than that of pure C18. The thermal conductivity of C1-C9 CPCM increased linearly with the increase of M-NPs@CNTs, indicating that the addition of M-NPs@CNTs significantly enhanced the thermal conductivity of the composite material, implying that the M-NPs@CNTs is an excellent thermally conductive filler that can be used to improve the thermal conductivity of CPCM.

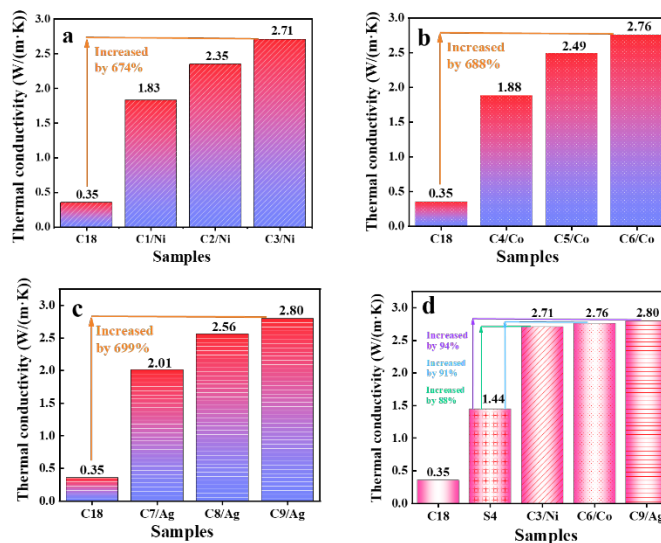


Fig. 7 Thermal conductivity of C18, C1-C9

Fig. 7(a) shows the effect of different NiNPs@CNTs doping amounts on the thermal conductivity of C18/NiNPs@CNTs/NF composite phase change materials. The thermal conductivity of C18/NiNPs@CNTs/NF phase change materials showed a significant increasing trend after NiNPs@CNTs doping; when the NiNPs@CNTs doping amount was 10 wt% (wt, mass fraction, the same hereafter), the thermal conductivity of CPCM increased to 2.71 W/mK, which is an increase of 674%. The effect of CoNPs@CNTs doping on the thermal conductivity of the thermal conductivity of C18/CoNPs@CNTs/NF composite phase change materials is shown in Fig. 7(b). The thermal conductivity of C18/CoNPs@CNTs/NF phase change materials also showed a significant increasing trend after doping with CoNPs@CNTs; when the doping amount of CoNPs@CNTs was 10 wt%, the thermal conductivity of CPCM increased to 2.76 W/mK, which was an increase of 688%. Finally, the effect of AgNPs@CNTs doping on the thermal conductivity of C18/AgNPs@CNTs/NF composite phase change materials was tested, as shown in Fig. 7(c). From the figure, it can be seen that the thermal conductivity of C18/AgNPs@CNTs/NF phase change material also shows a significant increasing trend after doping with AgNPs@CNTs; when the doping amount of AgNPs@CNTs is 10 wt%, the thermal conductivity of the CPCM increases to 2.80 W/mK, which is an increase of 699%. The results indicate that M-NPs@CNTs with high thermal conductivity can significantly enhance the thermal conductivity of the C18/M-NPs@CNTs/NF composite phase change material, which results in a more sensitive thermal response property and thus accelerates the storage or release of thermal energy. The thermal conductivity of CPCM is best when the doped thermally conductive filler is AgNPs@CNTs, and the thermal conductivities of the samples are all larger than those of CPCM doped with the thermally conductive fillers of NiNPs@CNTs and CoNPs@CNTs. The reason may be due to the fact that all of the thermal conductivity of AgNPs is larger than that of the other two types of M-NPs@CNTs, and so the thermal conductivities of the composite materials are larger after the addition.

It is worth noting that the improvement of thermal conductivity of CPCMs does not reach the expected magnitude, and the increase of thermal conductivity has been significantly slowed down when the doping amount of M-NPs@CNTs is increased from 5 wt% to 10 wt%. The reason for this is, on the one hand, because the specific surface area of M-NPs@CNTs is very large, although after ultrasonic dispersion treatment, but with the increase of its doping amount, it is inevitable that the phenomenon of CNTs agglomeration will occur, which slows down the increase of thermal conductivity of the composite phase-change materials; on the other hand, the agglomerated M-NPs@CNTs will be stacked up together, so that the surface structure of the material will become rough, which will increase the interfacial thermal conductivity of the material system to a certain extent. On the other hand, the surface structure of M-NPs@CNTs will become rougher after agglomeration, which will increase the interfacial thermal resistance of the material system to a certain extent, thus hindering the internal heat transfer of the hybrid system.

4. Conclusions

In summary, we successfully prepared a C18/M-NPs@CNTs/NF stereotypes composite phase change material by using NF as the support material, C18 as the phase change material, and M-NPs@CNTs as the thermal conductivity additive through vacuum impregnation and melt blending processes. M-NPs@CNTs, as an additive to improve thermal conductivity, in the synergistic effect of NF, the thermal conductivity of the C18/10wt%AgNPs@CNTs/NF composite material increased to 2.80W/(m·K), which was 699% higher than that of pure C18, while the phase change latent heat value of the composite material doped with 10wt%AgNPs@CNTs reached 160.5J/g, with a high phase change latent heat value. At the same time, M-NPs@CNTs also enhanced the thermal stability of the composite material.

References

- [1] J. Jacob, A.K. Pandey, N.A. Rahim, J. Selvaraj, M. Samykano, R. Saidur, V.V. Tyagi, “ Concentrated Photovoltaic Thermal (CPVT) systems: Recent advancements in clean energy applications, thermal management and storage”, vol.45, pp.103369, 2022.
- [2] T. Yang, W.P. King, N. Miljkovic, “Phase change material-based thermal energy storage”, *Cell Rep. Phys. Sci.* vol.2 , pp.100540,2021.
- [3] Y. Li, C. Li, N. Lin, B. Xie, D. Zhang, J. Chen, “Review on tailored phase change behavior of hydrated salt as phase change materials for energy storage”, *Mater. Today Energy.* Vol.22,pp.100866,2021.
- [4] W. Aftab, A. Usman, J. Shi, K. Yuan, M. Qin, R. Zou, “Phase change material-integrated latent heat storage systems for sustainable energy solutions”, *Energy Environ. Sci.* vol.14,pp.4268–4291,2021.
- [5] J.B.Xiao, B. Zou, Y.J. Zhuang, “Research and application on thermal conduction performance of metal foam composite phase change system”, *J. Central South University (Science and Technology)*, vol. 53, no.12, pp.4687–4699,2022.
- [6] D.H.Hu, X.Y. Xu, K. Lin, “Study on Heat Conductivity of Paraffin/Expanded Graphite/Graphite Sheet Composite Material”. *J. Eng Thermophys.* 2021.
- [7] Z. Yu, D. Feng, Y. Feng, X. Zhang, “Thermal conductivity and energy storage capacity enhancement and bottleneck of shape-stabilized phase change composites with graphene foam and carbon nanotubes”, *Compos. Part Appl. Sci. Manuf.* Vol.152, pp. 106703,2022.
- [8] Z. Xu, J. Hou, S. Q. Wan, “Preparation and thermal properties of metal foam/paraffin composite phase change materials”, *Energy Storage Sci. Tech.*, vol.9, no. 01pp.109-116,2020.
- [9] Y. Chen, Y.X. Ye, W. J. Du, “Heat transfer enhancement performance in phase change process of molten salt using foam metal”, *Chem Indu Eng Prog*, vol. 39, no.7,pp. 2566–2573,2020.
- [10] M.S. Zhu, Z. L. Wang, X.X.Sun, “Experimental research on effect of copper metal foam proportion on paraffin wax melting and heat transfer mechanism under high cell density”, *Chem Indu Eng Prog*, vol. 41, no.6, pp. 3203–3211,2022.
- [11] Z.J. Zhou, Z.H.Hu, M.Yang, “Effect of Contact Gap and Solidification for Metal Foam Composite PhaseChange Materials”. *J. Eng Therm.* 2022.

- [12] S. Zhang, D. Feng, L. Shi, L. Wang, Y. Jin, L. Tian, Z. Li, G. Wang, L. Zhao, Y. Yan, "A review of phase change heat transfer in shape-stabilized phase change materials (ss-PCMs) based on porous supports for thermal energy storage", *Renew. Sustain. Energy Rev.* vol.135, pp.110127,2021.
- [13] M. X. Diao, C. H. Guo, H. B. Gao, "Research progress in metal foam composites", *J. Mater Eng*, vol.50, no.12, pp.60-70,2022.
- [14] B. Lin, Z. H. Ju, D. H. Hu,"Thermal performance study of high thermal conductivity composite phase change thermal storage material based on copper foam skeleton", *Materials Reports*, vol.36, pp.21110168-5,2022.
- [15] J.J. Wang Jingjing, X.L.Xu, K. Y. Liang, "Research progress on heat transfer performance enhancement of porous-based shaped composite phase change materials", *J. Mater Eng*, vol, 42, no.1, pp. 26–38,2021.